

RESPONSE TO REVIEWER 1

Thank you for your comments.

1. In the section describing IMS-dataset you might want to explain a bit more in detail what instruments the dataset is based on.

IMS uses an often-changing list of instruments and models to build its dataset. We have added some examples of instruments that are used in Section 2.1.1.

Line 100: “The maps are produced by a trained analyst using visible imagery from a collection of geostationary (e.g. GOES, MeteoSat) and polar orbiting (e.g. AVHRR, MODIS, SAR) satellite instruments, with additional information from microwave sensors (e.g. DMSP, AMSR, AMSU), surface observations (e.g. SNOTEL), and models (e.g. SNODAS) (Helfrich et al., 2007).”

2. There is a fractional snow extent product from Globsnow/Sen3app projects that might be also worth a look and included in the comparison. For 2015 it is based on VIIRS (Suomi-NPP) data. The data and information are available here:

<http://www.globsnow.info/index.php?page=SE> or here:

http://sen3app.fmi.fi/index.php?page=Fractional_Snow_Cover_Extent_-_NH&style=main

We have looked at the fractional snow extent product from Globsnow/Sen3app as suggested, and have decided to exclude it from this work. This product does not provide snow cover information when clouds are present in the VIIRS observations. As a result, there is no information on snow cover for approximately a third of the TEMPO domain in 2015. Therefore, the product is not appropriate for the study performed here.

3. In the conclusion you write: “However, the lack of confidence in snow identification has previously led many retrieval procedures to omit observations over snow. Increasing this confidence such that these observations could be included would not only improve spatial and temporal sampling, but also allow the inclusion of observations with higher quality information on the lower troposphere.” It would be useful to actually demonstrate this with an example or case study, perhaps based on OMI data. I mean, showing one OMI scene/orbit of NO₂ retrievals, where the added value of this improved snow information would be visible. For example, an OMI orbit with snow-cover that was filtered out or somehow incorrectly flagged and would be improved using a more accurate knowledge of the snow cover (with the right AMFs and profiles) in the NO₂ retrieval.

Thank you for this suggestion. We have included a figure (Figure 6) that shows how including observations over snow improves sampling and increases AMFs. This is explained in the text on Line 280 as follows:

“We next examine the effect on both spatial sampling and sensitivity to the lower troposphere of a retrieval data set if observations with surface snow are included rather than omitted. We use IMS to identify the presence of snow for OMI observations over North America

in January 2015. We then use LIDORT to calculate AMFs for these observations using the corresponding snow-free (Sun et al., 2017) or snow-covered (O’Byrne et al., 2010) surface reflectance, and examine the results of either including or omitting snow-covered scenes. Figure 6 shows that including snow-covered scenes results in a significant (factor of 2.1) increase in observation frequency, particularly in the northern US and Canada. Additionally, including snow-covered scenes increases the average AMF by a factor of 2.7 in regions with occasional snow cover. The increase in AMF demonstrates that including snow-covered scenes increases the quality of information about the tropospheric NO₂ column by increasing the observation sensitivity to tropospheric NO₂.”

4. Could you comment on how the increased sensitivity in the PBL might affect NO₂ retrievals at relatively higher latitudes (where snow is very often present)? For example, how would those scattering weight profiles in Fig. 2 look like for higher SZA/or a different latitude? It might be less important for TEMPO but it is relevant for OMI/TROPOMI missions to improve retrieval at high latitudes in autumn-winter.

We have added a scattering weight profile for a high latitude location in Figure 2.

5. There is this paper by Vasilkov et al. about BRDF and OMI retrievals you might need to mention/discuss in your paper: Vasilkov, A., Qin, W., Krotkov, N., Lamsal, L., Spurr, R., Haffner, D., Joiner, J., Yang, E.-S., and Marchenko, S.: Accounting for the effects of surface BRDF on satellite cloud and trace-gas retrievals: a new approach based on geometry-dependent Lambertian equivalent reflectivity applied to OMI algorithms, *Atmos. Meas. Tech.*, **10, 333-349, <https://doi.org/10.5194/amt-10-333-2017>, 2017.**

We have added a mention to this paper in the introduction (Line 59):

“Correspondingly, surface snow may be mistaken for cloud, leading to errors in cloud fraction and pressure estimates used in trace gas retrievals (Lin et al., 2015; O’Byrne et al., 2010; Vasilkov et al., 2017).”

and in the conclusion, as follows (Line 316):

“This could potentially include Bidirectional Reflectance Distribution Functions (BRDF) that describe reflection at different viewing angles, as this effect has been shown to have significant impact on retrieved NO₂ columns (Vasilkov et al., 2017)”

RESPONSE TO REVEIWER 2

Thank you for your comments.

1. The assessment of different snow cover data sets is carried out for the entire year of 2015. This approach of using the full year data may cause biases in the metrics. The authors admit “All data sets have high accuracy numbers, owing to a high number of true negatives during the summer months” (Line 220). I think that the assessment of the snow cover data sets should be done on a seasonal basis and the metrics for different seasons should be compared. It would be particularly interesting to assess the snow data sets for spring when melting snow occurs.

We have included a table in the Appendix that gives evaluations of the snow data sets by season, and now include the following text on Line 245:

“Data sets were also evaluated by season with similar results (Appendix Table A1). All data sets have weaker performance metrics during the spring melt season, which has been observed in past evaluations (Frei et al., 2012). IMS has the highest F score in winter and autumn but is slightly outperformed by MAIAC in spring.”

However, keeping in mind that the goal of this work is to evaluate data sets for informing retrieval algorithms, and as most retrieval algorithms would likely choose a single data set to provide snow information throughout the year, we continue to focus on the full year data.

2. In my opinion, results of the RT simulations shown in Fig. 2 and 3 do not provide new significant information. Effects of surface reflectance on trace gas retrievals have been studied theoretically (see O’Byrne et al., JGR, 2010; Lin et al., ACP, 2015; Vasilkov et al., 2017 and references there).

We respectfully contend that Figures 2-3 do provide important information here. They illustrate how changes in snow cover affect the observation sensitivity to NO_2 . Indeed Reviewer 1 expressed interest in Figure 2.

Figure 2 of the manuscript (showing the scattering weights for a single solar zenith angle and a single NO_2 profile) is not conclusive because the NO_2 sensitivity to surface reflectance substantially depends on tropospheric NO_2 profiles (see Fig. 13 in Vasilkov et al., AMT, 2017).

It is true that the *column NO_2 sensitivity* depends on tropospheric NO_2 profiles. However, the scattering weights in Figure 2 represent the *sensitivity of backscattered radiation* to surface reflectance, which is independent of NO_2 profile. We have taken care to clarify this in the text (Line 201):

“Figure 2 shows the sensitivity of backscattered radiation (scattering weights) over snow-covered and snow-free surfaces ...”

Figure 3 compares AMFs for snow-covered and snow-free conditions for January 2013. The snow-free conditions are absolutely unrealistic for January. That is why I doubt that useful information can be derived from this comparison.

We clarified that the figure is for the observation geometry of January. The Figure 3 “snow-free conditions” plot shows AMF values in the case that snow is not present during a given observation. It is not meant to suggest that snow is never present in January in North America. As snow-covered scenes are often omitted in retrieval algorithms, the resulting data sets are essentially “snow-free”, and thus a snow-free map of AMF does provide important context.

I think that the text and figures related to the RT simulations can be removed without the loss of significant material. To some extent, this is supported by the title of the manuscript because the RT simulations are not mentioned in the title.

We have strengthened the material covering snow and AMFs by including Figure 6, which shows how including snow-covered scenes improves the quantity and quality of retrieval data sets. We have changed the title to reflect this as well. Together with Figures 2-3 we feel that this is new, significant information.

Specific comments Line 24. The quantity “F” is not defined here.

We have removed the mention of F here. It is defined later in the abstract.

Line 52. It is worthwhile to mention that uncertainties in surface reflectance also lead to uncertainties in the cloud fraction and pressure retrievals which affect the NO₂ retrievals (Vasilkov et al., AMT, 2017).

We now mention this effect in the introduction (Line 59):

“Correspondingly, surface snow may be mistaken for cloud, leading to errors in cloud fraction and pressure estimates used in trace gas retrievals (O’Byrne et al., 2010; Lin et al., 2015; Vasilkov et al., 2017).”

Line 162. Indeed, snow reflectivity is almost spectrally independent in UV/Vis. However, the maps in Fig. 1 include snow-free regions. For such regions, ground reflectivity does depend on wavelength, so reflectivity at 354 nm may not be used for 440 nm.

The snow reflectivity (for 354 nm) is only used when snow is present. Snow-free regions use the MODIS CMG Gap-Filled Snow-Free Products at 470 nm, which are at a wavelength closer to the 440 nm used in the AMF calculation. We have clarified this in the text and in Figure 1.

Line 174. Please clarify “the most reliable source is used”.

As stated, the GHCN-D data set includes information from multiple sources. GCHN-D provides a priority ranking of these sources. We have added a citation to this line which provides additional information.

Line 185. Please explain why the F score is most relevant for TEMPO.

This is now clarified in the text (Line 192) as follows:

“The F score balances recall (which accounts for false negatives) and precision (which accounts for false positives) to measure correct classification of snow without the influence of frequent snow-free periods, and therefore is the metric which is most relevant for TEMPO”

Line 190. Where does the OMI cloud fraction come from? How is the cloud fraction determined for snow-covered and partially snow-covered scenes?

We no longer use the OMI cloud fraction in this work. From line 199:

“We assume cloud-free conditions in the AMF calculations, as the impact of surface reflectance on retrieved cloud fractions is beyond the scope of this paper.”

Line 235. Is it correct that the MODIS products perform better at coarser resolution? Table 1 shows $F=0.46$ and 0.54 for the 4 km resolution while Table 2A shows $F=0.45$ and 0.53 for the 25 km resolution.

Yes, MODIS products do perform better when regridded to 4km than at their native resolution of 0.05° , where $F=0.37$ and 0.43 . However as pointed out by the reviewer, the benefit of regridding does not continue to improve if the resolution is further decreased. This has been clarified in the text (Line 250):

“...MODIS Aqua and Terra products perform better when regridded from their native 0.05° resolution to a 4 km resolution as it reduces the number of grid boxes missing observations due to cloud...”

Reference to McLinden et al., ACP, 2014 is missing.

This has been fixed.

Figure 1. The caption states “reflectivity at visible wavelengths”. The 354 nm wavelength (used for the upper panel) is not a visible wavelength. The lower panel is not informative because the color scale is not appropriate for it.

The figure caption now specifies “UV-Visible” instead of only “visible” wavelengths. We have also changed the colour scale.

Figure 2. The corresponding NO₂ profiles should be shown. Surface reflectivities should be specified. What is the viewing zenith angle of observations?

Surface reflectivities and zenith angles are now included in Figure 2. We have edited the text at Line 201 to better distinguish between the sensitivity of backscattered radiation to lower troposphere NO₂ (i.e. scattering weights) and the sensitivity of the NO₂ column to lower troposphere NO₂ (i.e. AMFs). Figure 2 focuses on how the scattering weights themselves (which do not depend on the NO₂ profile) are affected by reflectivity, and thus we do not include the corresponding NO₂ profiles for the sake of clarity.

“Figure 2 shows the sensitivity of backscattered radiation (scattering weights) over snow-covered and snow-free surfaces for two locations ... This shows that satellite observed backscattered radiation is up to five times as sensitive to NO₂ in the boundary layer in the presence of snow, due to the increased absorption by NO₂ in the lower troposphere when the surface reflects more sunlight.”

Appendix. Please explain why some numbers for the CMC and NISE data sets are slightly different in Tables A1 and A2. The spatial resolution of the data sets is same for both tables.

Thank you for noticing this. There were some errors in the Appendix tables that have been corrected. In Table A3 (previously A2), all products were regridded to a common 25km

resolution. For NISE, this is slightly different than its native 25km grid, hence a small difference in its F score (0.51 to 0.52).

1 **Assessing snow extent data sets over North America to inform and improve trace gas**
2 **retrievals from solar backscatter**

3 Matthew J. Cooper¹, Randall V. Martin^{1,2}, Alexei I. Lyapustin³, and Chris A. McLinden⁴

4 1. Department of Physics and Atmospheric Science, Dalhousie University, Halifax, Nova Scotia,
5 Canada.

6 2. Harvard-Smithsonian Center for Astrophysics, Cambridge, Massachusetts, USA

7 3. NASA Goddard Space Flight Center, Greenbelt, MD, USA

8 4. Air Quality Research Division, Environment and Climate Change Canada, Toronto, Ontario,
9 Canada

10 **Abstract**

11 Accurate representation of surface reflectivity is essential to tropospheric trace gas retrievals
12 from solar backscatter observations. Surface snow cover presents a significant challenge due to
13 its variability and thus snow-covered scenes are often omitted from retrieval data sets; however,
14 the high reflectance of snow is advantageous for trace gas retrievals. We first examine the
15 implications of surface snow on retrievals from the upcoming TEMPO geostationary instrument
16 for North America. We use a radiative transfer model to examine how an increase in surface
17 reflectivity due to snow cover changes the sensitivity of satellite retrievals to NO₂ in the lower
18 troposphere. We find that a substantial fraction (>50%) of the TEMPO field of regard can be
19 snow covered in January, and that the average sensitivity to the tropospheric NO₂ column
20 substantially increases (doubles) when the surface is snow covered.

21 We then evaluate seven existing satellite-derived or reanalysis snow extent products against
22 ground station observations over North America to assess their capability of informing surface
23 conditions for TEMPO retrievals. The Interactive Multisensor Snow and Ice Mapping System
24 (IMS) had the best agreement with ground observations (accuracy=93%, precision=87%,
25 recall=83%, ~~F=85%~~). Multiangle Implementation of Atmospheric Correction (MAIAC)
26 retrievals of MODIS observed radiances had high precision (90% for Aqua and Terra), but
27 underestimated the presence of snow (recall=74% for Aqua, 75% for Terra). MAIAC generally
28 outperforms the standard MODIS products (precision=51%, recall=43% for Aqua;

29 precision=69%, recall=45% for Terra). The Near-real-time Ice and Snow Extent (NISE) product
30 had good precision (83%) but missed a significant number of snow covered pixels (recall=45%).
31 The Canadian Meteorological Centre (CMC) Daily Snow Depth Analysis Data set had strong
32 performance metrics (accuracy=91%, precision=79%, recall=82%, ~~$F=81%$~~). We use the F score,
33 which balances precision and recall, to determine overall product performance ($F = 85%$,
34 82(82)%, 81%, 58%, 46(54)% for IMS, MAIAC Aqua(Terra), CMC, NISE, MODIS
35 Aqua(Terra) respectively) for providing snow cover information for TEMPO retrievals from
36 solar backscatter observations. We find that using IMS to identify snow cover and enable
37 inclusion of snow-covered scenes across North America in January can increase both the number
38 of observations by a factor of 2.1 and the average sensitivity to the tropospheric NO₂ column by
39 a factor of 2.7.

40

41 1. Introduction

42 Satellite observations of solar backscatter are widely used as a source of information on
43 atmospheric trace gases (Richter and Wagner, 2011). These observations have provided valuable
44 information on vertical column densities of O₃, NO₂, SO₂, CO, HCHO, CH₄ and other important
45 trace gases in the troposphere (Fishman et al., 2008). Satellite observations of trace gases have
46 been used to assess air quality (Duncan et al., 2014; Martin, 2008) and to gain insight into
47 atmospheric processes including emissions (Streets et al., 2013), lifetimes (Beirle et al., 2011;
48 Fioletov et al., 2015; de Foy et al., 2015; Valin et al., 2013), and deposition (Geddes and Martin,
49 2017; Nowlan et al., 2014). The utility of these observations is dependent on their quality, and
50 thus ensuring retrieval accuracy is essential.

51 Previous studies have found that retrieved NO₂ vertical column densities are highly
52 sensitive to errors in assumed surface reflectance (Boersma et al., 2004; Lamsal et al., 2017;
53 Martin et al., 2002). Much of this error sensitivity results from observation sensitivity to trace
54 gases in the lower troposphere. The observation sensitivity is accounted for in the air mass factor
55 (AMF) conversion of observed line-of-sight “slant columns” to vertical column densities.
56 Uncertainties in surface reflectance are a significant contributor to AMF uncertainty.

57 Existing reflectivity climatologies (e.g. Kleipool et al., 2008; Koelemeijer et al., 2003;
58 Liang et al., 2002; Herman and Celarier, 1997) do not represent snow cover well, since the
59 statistical methods to exclude reflective clouds from the climatologies also exclude variable
60 snow cover; Correspondingly, surface snow may be mistaken for cloud, leading to errors in
61 cloud fraction and pressure estimates used in trace gas retrievals (Lin et al., 2015; O’Byrne et al.,
62 2010; Vasilkov et al., 2017). Therefore, snow cover is particularly challenging to retrievals.
63 Misrepresenting surface snow cover can lead to large errors (20-50%) in retrieved NO₂ columns
64 over broad regions with seasonal snow cover (O’Byrne et al., 2010). For this reason,
65 observations over snow are often omitted to avoid potential errors. This limits the ability of
66 satellite retrieved data sets to offer adequate temporal and spatial sampling in winter months.
67 Additionally, over highly reflective surfaces such as snow observation sensitivity to the lower
68 troposphere is larger and has less dependence on *a priori* NO₂ profiles ~~over highly reflective~~
69 ~~surfaces such as snow~~ (Lorente et al., 2017; O’Byrne et al., 2010); Thus, omitting snow-covered
70 scenes means omitting the observations with the greatest sensitivity to the lower troposphere.
71 This could be remedied by using a product that would allow for snow cover identification to be
72 done with confidence.

73 Several data products provide information on snow extent using surface station
74 observations, satellite observed radiances, or visible imagery. Previous evaluations have found it
75 difficult to determine which of these products is definitively the best, partly due to differences in
76 resolution. Most products are more consistent during the winter months when persistent, deep
77 snow is present (Frei et al., 2012; Frei and Lee, 2010). However, disagreements are common
78 during accumulation and melting seasons, over mountains, and under forest canopies. These
79 evaluations have largely focused on local or regional snow cover, or included only cloud-free
80 observations.

81 The upcoming geostationary Tropospheric Emissions: Monitoring of Pollution (TEMPO)
82 satellite instrument will provide hourly observations of air quality relevant trace gases over
83 North America at an unprecedented spatial and temporal resolution (Zoogman et al., 2017). As is
84 the case for all nadir satellite retrievals, the quality of these observations will depend on the
85 accuracy of the surface reflectance used in the retrieval. As a significant portion of the observed

86 domain experiences snow cover, an accurate representation of snow cover is needed. Current
87 plans to deal with snow cover for TEMPO are to rely on external observations.

88 In this work, we examine the importance of accurate snow identification by using a
89 radiative transport model to evaluate how the vertical sensitivity of a satellite retrieval is
90 impacted by surface reflectance. We then assess seven snow extent products that are expected to
91 continue to be operational during the TEMPO mission using in situ observations across North
92 America with the intent of determining which product is best suited for providing snow cover
93 information for TEMPO and other future satellite retrievals. Finally, we combine radiative
94 transfer model results with a snow extent product to show how including snow-covered scenes
95 improves both the quantity and quality of information in a retrieval data set.

96

97 **2. Data and Algorithms**

98 **2.1. Gridded Snow Products**

99 **2.1.1. IMS**

100 One of the most widely used sources of snow extent data is the Interactive Multisensor
101 Snow and Ice Mapping System (IMS). IMS provides daily, near-real-time maps of snow and sea
102 ice cover in the Northern Hemisphere at 4km resolution (Helfrich et al., 2007). The maps are
103 produced by a trained analyst using visible imagery from a collection of geostationary (e.g.
104 GOES, MeteoSat) and polar orbiting (e.g. AVHRR, MODIS, SAR) satellite instruments, with
105 additional information from microwave sensors (e.g. DMSP, AMSR, AMSU), surface
106 observations (e.g. SNOTEL), and models (e.g. SNODAS) (Helfrich et al., 2007). By using
107 multiple sources of information with different spatial resolution and temporal sampling, IMS can
108 minimize interference from clouds.

109 **2.1.2. MODIS**

110 A second commonly used snow and ice product is derived from MODIS satellite
111 observations from the Terra and Aqua satellites (Hall and Riggs, 2007). Terra and Aqua have
112 sun-synchronous, near polar orbits with overpass times of 1030 and 1330 hr respectively. Snow
113 cover is calculated using a Normalized Difference Snow Index (NDSI), which examines the

114 difference between observed radiation at visible wavelengths (where snow is highly reflective)
115 and short IR wavelengths (where there is little reflection from snow). Observations are made at
116 500 m spatial resolution and aggregated to produce daily snow cover fractions on a 0.05°
117 resolution grid. Past evaluations of the standard MODIS snow product show good agreement in
118 cloud-free conditions but often snow is misidentified as cloud (Hall and Riggs, 2007; Yang et al.,
119 2015).

120 The Multiangle Implementation of Atmospheric Correction (MAIAC) algorithm is ~~also~~
121 ~~derived from another algorithm processing~~ MODIS observations. MAIAC retrievals uses
122 radiances observed by the MODIS Aqua and Terra satellites to provide atmospheric and surface
123 products including snow detection on a 1 km grid (Lyapustin et al., 2011a, 2011b, 2012). While
124 the NDSI used by the standard MODIS product is also used by MAIAC as one of the criteria, the
125 overall snow and cloud detection in MAIAC are different from the standard MODIS algorithm
126 (Lyapustin et al., 2008).

127 **2.1.3. NISE**

128 The Near-real-time Ice and Snow Extent (NISE) provides daily updated snow cover
129 extent information on a 25x25 km grid (Nolin et al., 2005). NISE uses microwave measurements
130 from the Special Sensor Microwave Imager/Sounder (SSM/I) on a sun-synchronous, quasi-polar
131 orbit to observe how microwave radiation emitted by soil is scattered by snow. Products based
132 on microwave measurements such as NISE are known to miss wet and thin snow, as wet snow
133 emits microwave radiation similar to soil, and thin snow does not provide sufficient scattering.

134 **2.1.4. CMC**

135 The Canadian Meteorological Centre (CMC) Daily Snow Depth Analysis Data is a
136 statistical interpolation of snow depth measurements from 8,000 surface sites across Canada and
137 U.S. interpolated using a snow pack model (Brasnett, 1999). Unlike the aforementioned satellite
138 products that provide snow extent, CMC provides snow depths. Daily snow maps are produced
139 at 25 km resolution. As it a reanalysis product, there is a time delay in availability. The CMC
140 snow depths show good agreement with independent observations over midlatitudes and is
141 considered an improvement over previous snow depth climatologies (Brown et al., 2003).

142 **2.2 Surface observations**

143 These snow identification products are evaluated against surface station observations
144 from the Global Historical Climatology Network-Daily (GHCN-D) database, an amalgamation
145 of daily climate records from over 80,000 surface stations worldwide (Menne et al., 2012a).
146 Most observations over Canada and the United States are collected by government organizations
147 (Environment and Climate Change Canada and NOAA National Climatic Data Center,
148 respectively) with additional measurements from smaller observation networks. While the focus
149 of the database is collecting temperature and precipitation measurements, many stations (1,279 in
150 Canada, 13,932 in United States in 2015 used here) also offer snow depth measurements.

151 A subset of the surface stations included in GHCN-D may also be used in the CMC
152 reanalysis. It is difficult to definitively know which stations are used, as CMC does not routinely
153 archive this information. However, we estimate that only 5% of the GHCN-D stations used here
154 are located within 0.1° of a possible CMC station, and thus GHCN-D has sufficient independent
155 information sources to evaluate the CMC product.

156 **2.3 Radiative transfer calculations**

157 The sensitivity of satellite observations of NO_2 to its vertical distribution is calculated
158 here using the LIDORT radiative transfer model (Spurr, 2002). The model is used to calculate
159 scattering weights, which quantify the sensitivity of backscattered solar radiation to NO_2 at
160 different altitudes (Martin et al., 2002; Palmer et al., 2001). The observation sensitivity to lower
161 tropospheric NO_2 is represented by the air mass factor. Air mass factors for OMI satellite
162 observations in January 2013 are calculated as a useful analog for future TEMPO observations as
163 both instruments are spectrometers observing reflected sunlight at UV to visible wavelengths.
164 AMFs are calculated at 440 nm, at the centre of the NO_2 retrieval window for OMI and TEMPO
165 where NO_2 has strong absorption features. Vertical NO_2 profiles, and other trace gas and aerosol
166 profiles needed for the AMF calculation shown here, are obtained from a simulation of the
167 GEOS-Chem chemical transport model version 11-01 (www.geos-chem.org).

168 Figure 1 shows maps of snow-free and snow-covered reflectances used here. Snow-free
169 surface reflectance [at 470 nm](#) is provided by Nadir BRDF-Adjusted reflectances from the
170 MODIS CMG Gap-Filled Snow-Free Products (Sun et al., 2017). Reflectivities at 354 nm for
171 snow-covered scenes are derived from OMI observations as described by O'Byrne et al. (2010).
172 While this wavelength is different than the 440 nm wavelength used to calculate AMFs, snow

173 reflectivity has weak spectral dependence in UV-Visible wavelengths (Feister and Grewe, 1995;
174 O’Byrne et al., 2010). Snow can increase surface reflectance by over a factor of 10 in central
175 North America where short vegetation is readily covered by snow.

176 **3. Methods**

177 Here we test daily snow cover products for 2015. Snow products are regridded from their
178 native resolutions to a common 4 km grid (similar to the spatial resolution of TEMPO). A grid
179 box is considered to be snow covered if any observations within that box are snow covered.
180 MAIAC, NISE, and IMS give only a yes/no flag for presence of snow. MODIS products provide
181 a pixel snow fraction, and we consider any pixels with nonzero snow fractions as snow covered.
182 Any CMC grid box with nonzero snow depth is considered snow covered.

183 GHCN-D surface measurements are used as the ground “truth” for evaluating the satellite
184 and reanalysis snow data products tested here. If measurements from multiple surface data
185 networks exist in the same grid box, the most reliable source is used per the priority order given
186 by GHCN-D (Menne et al., 2012b). If observations from multiple surface stations within the
187 most reliable network within a grid box disagree on the presence of snow on a given day, that
188 day is excluded from the evaluation.

189 We assess the snow data sets using metrics that are commonly used for evaluating binary
190 data sets (Rittger et al., 2013). These metrics are based on the possible outcomes for identifying
191 snow: true positive (TP), true negative (TN), false positive (FP), and false negative (FN).
192 Accuracy measures the likelihood that a grid box, with snow or without, is correctly classified:

$$Accuracy = \frac{TP + TN}{TP + TN + FP + FN} \quad (1)$$

193 Precision is the probability that a region identified as snow-covered has snow:

$$Precision = \frac{TP}{TP + FP} \quad (2)$$

194 Recall is the likelihood that snow cover is detected when present:

$$Recall = \frac{TP}{TP + FN} \quad (3)$$

195 The F score balances recall (which accounts for false negatives) and precision (which accounts
196 for false positives) to measure correct classification of snow without the influence of frequent
197 snow-free periods, and therefore is the metric which is most relevant for TEMPO:

$$F = 2 * \frac{\textit{precision} * \textit{recall}}{\textit{precision} + \textit{recall}} \quad (4)$$

198 4. Results

199 We first examine the effect of surface reflectivity on retrieval sensitivity by using the
200 LIDORT radiative transfer model to calculate NO₂ air mass factors for both snow-free and snow-
201 covered scenarios over North America. We calculate air mass factors ~~for all cloud free (OMI~~
202 ~~cloud fraction < 20%) OMI NO₂ observations~~ over North America in January 2013. We assume
203 cloud-free conditions in all AMF calculations, as the impact of surface reflectance on retrieved
204 cloud fractions is beyond the scope of this paper.

205 Figure 2 shows the sensitivity of backscattered radiation (scattering weights) over snow-
206 covered and snow-free ~~retrieval sensitivity (scattering weights) surfaces~~ for two locations; a
207 midlatitude location (in the US Midwest, 42°N, 100°W) with a solar zenith angle of 60° and
208 at a high latitude location (Northern Canada, 58°N, 76°W) with a solar zenith angle of 79°. The
209 ~~mean~~ snow-covered scattering weights are greater than the ~~mean~~ snow-free scattering weights
210 throughout the troposphere, by factors of 2.0 (2.7) below 5 km, 2.6 (3.7) below 2 km, and
211 3.2 (5.3) below 1 km at the mid (high) latitude location. This shows that ~~a~~ satellite observed
212 backscattered radiation is up to three-five times as sensitive to NO₂ in the boundary layer in
213 the presence of snow, due to the increased absorption by NO₂ in the lower troposphere when the
214 surface reflects more sunlight.

215 Figure 3 shows the distribution of AMF values over ~~the TEMPO field of regard~~ North
216 America with and without reflectance from snow. The snow-free AMF distribution is unimodal
217 with a median of 1.2. Allowing for the presence of snow introduces a second mode with a
218 median of 3.2. Mean AMFs increase by a factor 2.0 in the presence of snow, indicating an
219 overall doubling in the sensitivity to tropospheric NO₂ over snow covered surfaces across North
220 America. The impact is larger over polluted regions, as mean AMFs increase by a factor of 2.2 in
221 regions where NO₂ columns exceed 1x10¹⁵ molec/cm². Maps of AMF with and without snow

222 cover for January 2013 show that AMF values increase over 69% of the land surface within the
223 TEMPO domain.

224 We next examine the snow datasets to identify the one most suited for the TEMPO
225 retrieval algorithm. Figure 4 shows the spatial distribution of false positives and false negatives
226 in the data sets. In all data sets, both false positives and negatives are most frequent over
227 mountainous regions, particularly in the Rocky Mountain region, consistent with previous
228 validation studies (Chen et al., 2012, 2014; Frei et al., 2012; Frei and Lee, 2010). These errors
229 are often attributed to differences in representativeness, as snow cover in mountain regions is
230 often spatially inhomogeneous, and thus *in situ* measurements may not be representative of the
231 pixel. A slight increase in the number of false positives in IMS over mid-western and prairie
232 regions may result from crop regions with high snow-free albedos being mistaken for snow in
233 visible imagery (Chen et al., 2012; Yang et al., 2015). NISE, MODIS Aqua, and MODIS Terra
234 have more false negatives overall, especially in the Great Lakes and New England regions. False
235 positives are less frequent than false negatives in all data sets. IMS and CMC have the lowest
236 frequency of false negatives. NISE and MAIAC have the lowest frequency of false positives.

237 Figure 5 shows the metrics used to evaluate data set performance. Table 1 summarizes
238 these results. All data sets have high accuracy numbers, owing largely to a high number of true
239 negatives during the summer months. MODIS Aqua and Terra have low recall and *F* scores.
240 When only observations with MODIS cloud fractions less than 20% are used, MODIS has better
241 agreement with the ground stations (*F* statistic increases from 0.38 to 0.49 at native resolution
242 for Aqua, 0.43 to 0.63 for Terra), however this reduces the number of usable MODIS
243 observations by up to 60%. NISE has high precision but low recall, indicating that while areas
244 classified as snow-covered by NISE are likely correct, many snow-covered regions are missing
245 in the data set. This is consistent with evaluations by McLinden et al. (2014) and O’Byrne et al.
246 (2010). Although CMC, IMS, and MAIAC products show an increase in frequency of false
247 negatives over the Rocky Mountains, they retain a high precision in this region due to frequent
248 snow cover. While MAIAC Aqua/Terra have high accuracy and precision, lower recall values
249 indicate that they are conservative in identifying the presence of snow. This is possibly a
250 consequence of the method used for identifying cloud, which may incorrectly classify fresh
251 snowfall as cloud (Lyapustin et al., 2008). Data sets were also evaluated by season with similar

252 results (Appendix Table A1). All data sets have weaker performance metrics during the spring
253 melt season, which has been observed in past evaluations (Frei et al., 2012). IMS has the highest
254 F score in winter and autumn but is slightly outperformed by MAIAC in spring. Data sets were
255 also evaluated at their native resolutions and at a common 25 km resolution (Appendix Tables
256 A2-3). Results are similar at each resolution with two exceptions: MODIS Aqua and Terra
257 products perform better when regridded from their native 0.05° resolution to a 4 km coarser
258 resolution as it reduces the number of grid boxes missing observations due to cloud, and MAIAC
259 Aqua and Terra perform better at their native resolution than at either 4 km or 25 km as
260 degrading the spatial resolution results in a loss of information.

261 For all data sets, recall is generally low in two regions: along the Pacific coastline where
262 snow depths are relatively thin, and in the south when snow is rare and generally short lived.
263 Thin snow is likely to be less homogenous across a pixel and more likely to be obscured by
264 forest canopies or tall grasses, and thus is difficult to observe from satellite imagery. Short lived
265 snow in the south is likely to be missed by satellite observations, especially since clouds are
266 often present. However, as IMS uses multiple observations at multiple times of day in addition to
267 incorporating ground station data, it is more likely to find snow in these cases than other satellite
268 products (Hall et al., 2010). Overall, IMS has best agreement with *in situ* observations, with the
269 highest accuracy, recall, and *F* statistic and relatively high precision.

270 While CMC also has strong performance metrics, it is important to consider the
271 information source used to describe snow extent in each product. Products based on satellite
272 observations are advantageous when assessing how surface reflectivity affects backscattered
273 radiation observed from space. For example, thin snow, or snow obscured by tree canopies, may
274 not affect the observed brightness from space, but would be considered snow-covered by a
275 product based on surface observations (e.g. CMC). Also, the reflectivity of a snow-covered
276 surface decreases over time as the snow ages (Warren and Wiscombe, 1980); This effect would
277 not be captured by snow depth measurements. And while snow depth has been used as an
278 indicator of brightness (Arola et al., 2003), it can not account for snow aging or canopy effects.
279 IMS is based on visible satellite imagery and thus determines snow extent based on brightness
280 from space, which is more applicable to satellite retrievals. And while most satellite-based
281 products rely on observations made at a single overpass time and viewing geometry, IMS has the

282 advantage of incorporating observations from multiple satellites with differing measurement
283 times and geometries, including both geostationary and low Earth orbits. These reasons, in
284 addition to a strong agreement with in situ measurements and near-real-time updates, make IMS
285 best suited for informing TEMPO retrievals.

286 We next examine the effect on both spatial sampling and sensitivity to the lower
287 troposphere of a retrieval data set if observations with surface snow are included rather than
288 omitted. We use IMS to identify the presence of snow for OMI observations over North America
289 in January 2015. We then use LIDORT to calculate AMFs for these observations using the
290 corresponding snow-free (Sun et al., 2017) or snow-covered (O’Byrne et al., 2010) surface
291 reflectance, and examine the results of either including or omitting snow-covered scenes. Figure
292 6 shows that including snow-covered scenes results in a significant (factor of 2.1) increase in
293 observation frequency, particularly in the northern US and Canada. Additionally, including
294 snow-covered scenes increases the average AMF by a factor of 2.7 in regions with occasional
295 snow cover. The increase in AMF demonstrates that including snow-covered scenes increases
296 the quality of information about the tropospheric NO₂ column by increasing the observation
297 sensitivity to tropospheric NO₂.

298

299 5. Conclusion

300 An accurate representation of snow cover is essential to ensuring satellite retrieval
301 accuracy, including those from TEMPO. Radiative transfer model calculations indicate that NO₂
302 retrievals over reflective snow-covered surfaces are more than twice as sensitive to NO₂ in the
303 boundary layer than over snow-free surfaces, ~~with the greatest increases in sensitivity occurring~~
304 ~~over polluted regions~~. This makes snow an attractive surface over which to observe tropospheric
305 NO₂. However, the lack of confidence in snow identification has previously led many retrieval
306 procedures to omit observations over snow. We show that ~~h~~increasing this confidence such that
307 these observations could be included ~~would~~ not only improve ~~s~~ spatial and temporal sampling,
308 but also allow ~~s~~ the inclusion of observations with higher quality information on the lower
309 troposphere.

310 We evaluated seven snow extent data sets to determine their usefulness for informing
311 satellite retrievals of trace gas from solar backscatter observations. All products were more likely
312 to misidentify snow over mountains or where snow cover is thin or short lived. IMS had the best
313 agreement with *in situ* observations ($F=0.85$), and as a satellite based, operational, daily updated
314 product, it is well suited for informing TEMPO satellite retrievals. The low recall value (0.45)
315 for NISE indicated that a significant number of snow covered pixels are missed. The standard
316 MODIS products showed medium precision and low recall owing to cloud contamination. The
317 MAIAC products had the highest precision (0.90 for both Aqua and Terra) of those tested, but is
318 conservative in ascribing the presence of snow (recall=0.74 for Aqua, 0.75 for Terra). CMC had
319 strong performance metrics ($F=0.81$), but as a reanalysis product based on ground observations it
320 may not appropriately represent how a surface snow reflectivity would affect TEMPO observed
321 radiances.

322 Future work should investigate snow reflectance products, ~~potentially including~~
323 ~~Bidirectional Reflectance Distribution Functions (BRDF) that describe reflection at different~~
324 ~~viewing angles,~~ that could be used when snow is detected. This could potentially include
325 Bidirectional Reflectance Distribution Functions (BRDF) that describe reflection at different
326 viewing angles, as this effect has been shown to have significant impact on retrieved NO₂
327 columns (Vasilkov et al., 2017). A retrieval algorithm that combines daily snow detection from
328 IMS with a climatology of snow reflectance has the potential to greatly improve upon current
329 methodologies.

330

331 6. Data Availability

332 IMS (National Ice Center, 2008), NISE (Brodzik and Stewart, 2016), MODIS Aqua (Hall
333 and Riggs, 2016a), MODIS Terra (Hall and Riggs, 2016b), and CMC (Brown and Brasnett,
334 2010) data are available from the NASA National Snow and Ice Data Center (<http://nsidc.org>).
335 MAIAC Collection 6 re-processing of MODIS data started in September 2017 and is expected to
336 be completed by the end of year. This study used MAIAC data currently available via ftp at
337 NASA Center for Climate Simulations (NCCS):
338 <ftp://maiac@dataportal.nccs.nasa.gov/DataRelease/>. GHCN-D data are available from the
339 NOAA National Climatic Data Center (Menne et al., 2012b; www.ncdn.noaa.gov). Code for

340 calculating scattering weights and air mass factors, and snow-covered surface reflectances used
341 here are available at <http://fizz.phys.dal.ca/~atmos>. Snow-free surface reflectances are available
342 at <ftp://rsftp.eeos.umb.edu/data02/Gapfilled/>. The GEOS-Chem chemical transport model used
343 here is available at www.geos-chem.org.

344 **7. References**

- 345 Arola, A., Kaurola, J., Koskinen, L., Tanskanen, A., Tikkanen, T., Taalas, P., Herman, J. R.,
346 Krotkov, N. and Fioletov, V.: A new approach to estimating the albedo for snow-covered
347 surfaces in the satellite UV method, *J. Geophys. Res.*, 108(D17), 4531,
348 doi:10.1029/2003JD003492, 2003.
- 349 Beirle, S., Boersma, K. F., Platt, U., Lawrence, M. G. and Wagner, T.: Megacity emissions and
350 lifetimes of nitrogen oxides probed from space., *Science*, 333(6050), 1737–9,
351 doi:10.1126/science.1207824, 2011.
- 352 Boersma, K. F., Eskes, H. J. and Brinksma, E. J.: Error analysis for tropospheric NO₂ retrieval
353 from space, *J. Geophys. Res. Atmos.*, 109(D4), 2004.
- 354 Brasnett, B.: A Global Analysis of Snow Depth for Numerical Weather Prediction, *J. Appl.*
355 *Meteorol.*, 38(6), 726–740, doi:10.1175/1520-0450(1999)038<0726:AGAOSD>2.0.CO;2, 1999.
- 356 Brodzik, M. J. and Stewart, J. S.: Near-Real-Time SSM/I-SSMIS EASE-Grid Daily Global Ice
357 Concentration and Snow Extent, Version 5, , doi:<http://dx.doi.org/10.5067/3KB2JPLFPK3R>,
358 2016.
- 359 Brown, R. D. and Brasnett, B.: Canadian Meteorological Centre (CMC) Daily Snow Depth
360 Analysis Data, Version 1, , doi:<http://dx.doi.org/10.5067/W9FOYWH0EQZ3>, 2010.
- 361 Brown, R. D., Brasnett, B. and Robinson, D.: Gridded North American monthly snow depth and
362 snow water equivalent for GCM evaluation, *Atmosphere-Ocean*, 41(1), 1–14,
363 doi:10.3137/ao.410101, 2003.
- 364 Chen, C., Lakhankar, T., Romanov, P., Helfrich, S., Powell, A. and Khanbilvardi, R.: Validation
365 of NOAA-Interactive Multisensor Snow and Ice Mapping System (IMS) by Comparison with
366 Ground-Based Measurements over Continental United States, *Remote Sens.*, 4(12), 1134–1145,
367 doi:10.3390/rs4051134, 2012.

368 Chen, X., Jiang, L., Yang, J. and Pan, J.: Validation of ice mapping system snow cover over
369 southern China based on Landsat Enhanced Thematic Mapper Plus imagery, *J. Appl. Remote*
370 *Sens.*, 8(1), 84680, doi:10.1117/1.JRS.8.084680, 2014.

371 Duncan, B. N., Prados, A. I., Lamsal, L. N., Liu, Y., Streets, D. G., Gupta, P., Hilsenrath, E.,
372 Kahn, R. A., Nielsen, J. E., Beyersdorf, A. J., Burton, S. P., Fiore, A. M., Fishman, J., Henze, D.
373 K., Hostetler, C. A., Krotkov, N. A., Lee, P., Lin, M., Pawson, S., Pfister, G., Pickering, K. E.,
374 Pierce, R. B., Yoshida, Y. and Ziemba, L. D.: Satellite data of atmospheric pollution for U.S. air
375 quality applications: Examples of applications, summary of data end-user resources, answers to
376 FAQs, and common mistakes to avoid, *Atmos. Environ.*, 94, 647–662,
377 doi:10.1016/j.atmosenv.2014.05.061, 2014.

378 Feister, U. and Grewe, R.: Spectral albedo measurements in the UV and visible region over
379 different types of surfaces, *Photochem. Photobiol.*, 62(4), 736–744, doi:10.1111/j.1751-
380 1097.1995.tb08723.x, 1995.

381 Fioletov, V. E., McLinden, C. A., Krotkov, N. and Li, C.: Lifetimes and emissions of SO₂ from
382 point sources estimated from OMI, *Geophys. Res. Lett.*, 42(6), 1969–1976,
383 doi:10.1002/2015GL063148, 2015.

384 Fishman, J., Al-Saadi, J. A., Creilson, J. K., Bowman, K. W., Burrows, J. P., Richter, A.,
385 Chance, K. V., Edwards, D. P., Martin, R. V., Morris, G. A., Pierce, R. B., Ziemke, J. R.,
386 Schaack, T. K., Thompson, A. M., Fishman, J., Al-Saadi, J. A., Creilson, J. K., Bowman, K. W.,
387 Burrows, J. P., Richter, A., Chance, K. V., Edwards, D. P., Martin, R. V., Morris, G. A., Pierce,
388 R. B., Ziemke, J. R., Schaack, T. K. and Thompson, A. M.: Remote Sensing of Tropospheric
389 Pollution from Space, *Bull. Am. Meteorol. Soc.*, 89(6), 805–821,
390 doi:10.1175/2008BAMS2526.1, 2008.

391 de Foy, B., Lu, Z., Streets, D. G., Lamsal, L. N. and Duncan, B. N.: Estimates of power plant NO
392 x emissions and lifetimes from OMI NO₂ satellite retrievals, *Atmos. Environ.*, 116, 1–11, 2015.

393 Frei, A. and Lee, S.: A comparison of optical-band based snow extent products during spring
394 over North America, *Remote Sens. Environ.*, 114(9), 1940–1948, doi:10.1016/j.rse.2010.03.015,
395 2010.

396 Frei, A., Tedesco, M., Lee, S., Foster, J., Hall, D. K., Kelly, R. and Robinson, D. A.: A review of
397 global satellite-derived snow products, *Adv. Sp. Res.*, 50(8), 1007–1029,
398 doi:10.1016/j.asr.2011.12.021, 2012.

399 Geddes, J. A. and Martin, R. V.: Global deposition of total reactive nitrogen oxides from 1996 to
400 2014 constrained with satellite observations of NO₂ columns, *Atmos. Chem. Phys.*, 17(16),
401 10071–10091, doi:10.5194/acp-17-10071-2017, 2017.

402 Hall, D. . and Riggs, G. A.: MODIS/Aqua Snow Cover Daily L3 Global 0.05Deg CMG, Version
403 6, , doi:http://dx.doi.org/10.5067/MODIS/MYD10C1.006, 2016a.

404 Hall, D. K. and Riggs, G. A.: Accuracy assessment of the MODIS snow products, *Hydrol.*
405 *Process.*, 21(12), 1534–1547, doi:10.1002/hyp.6715, 2007.

406 Hall, D. K. and Riggs, G. A.: MODIS/Terra Snow Cover Daily L3 Global 0.05Deg CMG,
407 Version 6, , doi:http://dx.doi.org/10.5067/MODIS/MOD10C1.006, 2016b.

408 Hall, D. K., Fuhrmann, C. M., Perry, L. B., Riggs, G. A., Robinson, D. A. and Foster, J. L.: A
409 Comparison of Satellite-Derived Snow Maps with a Focus on Ephemeral Snow in North
410 Carolina, in 67th Eastern Snow Conference, Hancock MA USA., 2010.

411 Helfrich, S. R., McNamara, D., Ramsay, B. H., Baldwin, T. and Kasheta, T.: Enhancements to,
412 and forthcoming developments in the Interactive Multisensor Snow and Ice Mapping System
413 (IMS), *Hydrol. Process.*, 21(12), 1576–1586, doi:10.1002/hyp.6720, 2007.

414 Herman, J. R. and Celarier, E. A.: Earth surface reflectivity climatology at 340-380 nm from
415 TOMS data, *J. Geophys. Res. Atmos.*, 102(D23), 28003–28011, doi:10.1029/97JD02074, 1997.

416 Kleipool, Q. L., Dobber, M. R., de Haan, J. F. and Levelt, P. F.: Earth surface reflectance
417 climatology from 3 years of OMI data, *J. Geophys. Res.*, 113(D18), D18308,
418 doi:10.1029/2008JD010290, 2008.

419 Koelemeijer, R. B. A., de Haan, J. F. and Stammes, P.: A database of spectral surface reflectivity
420 in the range 335–772 nm derived from 5.5 years of GOME observations, *J. Geophys. Res.*,
421 108(D2), 4070, doi:10.1029/2002JD002429, 2003.

422 Lamsal, L. N., Janz, S. J., Krotkov, N. A., Pickering, K. E., Spurr, R. J. D., Kowalewski, M. G.,

423 Loughner, C. P., Crawford, J. H., Swartz, W. H. and Herman, J. R.: High-resolution NO₂
424 observations from the Airborne Compact Atmospheric Mapper: Retrieval and validation, *J.*
425 *Geophys. Res. Atmos.*, 122(3), 1953–1970, doi:10.1002/2016JD025483, 2017.

426 Liang, S., Fang, H., Chen, M., Shuey, C. J., Walthall, C., Daughtry, C., Morisette, J., Schaaf, C.
427 and Strahler, A.: Validating MODIS land surface reflectance and albedo products: methods and
428 preliminary results, *Remote Sens. Environ.*, 83(1–2), 149–162, doi:10.1016/S0034-
429 4257(02)00092-5, 2002.

430 Lin, J.-T., Liu, M.-Y., Xin, J.-Y., Boersma, K. F., Spurr, R., Martin, R. and Zhang, Q.: Influence
431 of aerosols and surface reflectance on satellite NO₂ retrieval: seasonal and spatial characteristics
432 and implications for NO_x emission constraints, *Atmos. Chem. Phys.*, 15(19), 11217–11241,
433 doi:10.5194/acp-15-11217-2015, 2015.

434 Lorente, A., Folkert Boersma, K., Yu, H., Dörner, S., Hilboll, A., Richter, A., Liu, M., Lamsal,
435 L. N., Barkley, M., De Smedt, I., Van Roozendaal, M., Wang, Y., Wagner, T., Beirle, S., Lin, J.-
436 T., Krotkov, N., Stammes, P., Wang, P., Eskes, H. J. and Krol, M.: Structural uncertainty in air
437 mass factor calculation for NO₂ and HCHO satellite retrievals, *Atmos. Meas. Tech.*, 10(3), 759–
438 782, doi:10.5194/amt-10-759-2017, 2017.

439 Lyapustin, A., Wang, Y. and Frey, R.: An automatic cloud mask algorithm based on time series
440 of MODIS measurements, *J. Geophys. Res.*, 113(D16), D16207, doi:10.1029/2007JD009641,
441 2008.

442 Lyapustin, A., Martonchik, J., Wang, Y., Laszlo, I. and Korkin, S.: Multiangle implementation of
443 atmospheric correction (MAIAC): 1. Radiative transfer basis and look-up tables, *J. Geophys.*
444 *Res.*, 116(D3), D03210, doi:10.1029/2010JD014985, 2011a.

445 Lyapustin, A., Wang, Y., Laszlo, I., Kahn, R., Korkin, S., Remer, L., Levy, R. and Reid, J. S.:
446 Multiangle implementation of atmospheric correction (MAIAC): 2. Aerosol algorithm, *J.*
447 *Geophys. Res.*, 116(D3), D03211, doi:10.1029/2010JD014986, 2011b.

448 Lyapustin, A. I., Wang, Y., Laszlo, I., Hilker, T., G.Hall, F., Sellers, P. J., Tucker, C. J. and
449 Korkin, S. V.: Multi-angle implementation of atmospheric correction for MODIS (MAIAC): 3.
450 Atmospheric correction, *Remote Sens. Environ.*, 127, 385–393, doi:10.1016/j.rse.2012.09.002,

451 2012.

452 Martin, R. V, Chance, K., Jacob, D. J., Kurosu, T. P., Spurr, R. J. D., Bucsela, E., Gleason, J. F.,
453 Palmer, P. I., Bey, I. and Fiore, A. M.: An improved retrieval of tropospheric nitrogen dioxide
454 from GOME, *J. Geophys. Res. Atmos.*, 107(D20), 2002.

455 Martin, R. V.: Satellite remote sensing of surface air quality, *Atmos. Environ.*, 42(34), 7823–
456 7843, doi:10.1016/j.atmosenv.2008.07.018, 2008.

457 McLinden, C. A., Fioletov, V., Boersma, K. F., Kharol, S. K., Krotkov, N., Lamsal, L., Makar,
458 P. A., Martin, R. V., Veefkind, J. P. and Yang, K.: Improved satellite retrievals of NO₂ and SO₂
459 over the Canadian oil sands and comparisons with surface measurements, *Atmos. Chem. Phys.*,
460 14(7), 3637–3656, doi:10.5194/acp-14-3637-2014, 2014.

461 Menne, M. J., Durre, I., Vose, R. S., Gleason, B. E., Houston, T. G., Menne, M. J., Durre, I.,
462 Vose, R. S., Gleason, B. E. and Houston, T. G.: An Overview of the Global Historical
463 Climatology Network-Daily Database, *J. Atmos. Ocean. Technol.*, 29(7), 897–910,
464 doi:10.1175/JTECH-D-11-00103.1, 2012a.

465 Menne, M. J., Durre, I., Korzeniewski, B., McNeal, S., Thomas, K., Yin, X., Anthony, S., Ray,
466 R., Vose, R. S., Gleason, B. E. and Houston, T. G.: Global Historical Climatology Network -
467 Daily (GHCN-Daily), Version 3.22, , doi:http://doi.org/10.7289/V5D21VHZ, 2012b.

468 National Ice Center: IMS Daily Northern Hemisphere Snow and Ice Analysis at 1 km, 4 km, and
469 24 km Resolutions, Version 1, , doi:http://dx.doi.org/10.7265/N52R3PMC, 2008.

470 Nolin, A., Armstrong, R. and Maslanik, J.: Near real-time SSM/I EASE-grid daily global ice
471 concentration and snow extent, *Digit. Media*, Natl. Snow Ice Data Center, Boulder, CO, USA,
472 2005.

473 Nowlan, C. R., Martin, R. V., Philip, S., Lamsal, L. N., Krotkov, N. A., Marais, E. A., Wang, S.
474 and Zhang, Q.: Global dry deposition of nitrogen dioxide and sulfur dioxide inferred from space-
475 based measurements, *Global Biogeochem. Cycles*, 28(10), 1025–1043,
476 doi:10.1002/2014GB004805, 2014.

477 O’Byrne, G., Martin, R. V., van Donkelaar, A., Joiner, J. and Celarier, E. A.: Surface reflectivity
478 from the Ozone Monitoring Instrument using the Moderate Resolution Imaging

479 Spectroradiometer to eliminate clouds: Effects of snow on ultraviolet and visible trace gas
480 retrievals, *J. Geophys. Res.*, 115(D17), D17305, doi:10.1029/2009JD013079, 2010.

481 Palmer, P. I., Jacob, D. J., Chance, K. and Martin, R. V: Air mass factor formulation for
482 spectroscopic measurements from satellites' Application to formaldehyde retrievals from the
483 Global Ozone Monitoring Experiment, *J. Geophys. Res.*, 106(D13), 14,514-539,550, 2001.

484 Richter, A. and Wagner, T.: The Use of UV, Visible and Near IR Solar Back Scattered Radiation
485 to Determine Trace Gases, pp. 67–121, Springer, Berlin, Heidelberg., 2011.

486 Rittger, K., Painter, T. H. and Dozier, J.: Assessment of methods for mapping snow cover from
487 MODIS, *Adv. Water Resour.*, 51, 367–380, doi:10.1016/j.advwatres.2012.03.002, 2013.

488 Spurr, R. J. D.: Simultaneous derivation of intensities and weighting functions in a general
489 pseudo-spherical discrete ordinate radiative transfer treatment, *J. Quant. Spectrosc. Radiat.*
490 *Transf.*, 75(75), 129–175 [online] Available from: www.elsevier.com/locate/jqsrt (Accessed 20
491 July 2017), 2002.

492 Streets, D. G., Canty, T., Carmichael, G. R., de Foy, B., Dickerson, R. R., Duncan, B. N.,
493 Edwards, D. P., Haynes, J. A., Henze, D. K. and Houyoux, M. R.: Emissions estimation from
494 satellite retrievals: A review of current capability, *Atmos. Environ.*, 77, 1011–1042, 2013.

495 Sun, Q., Wang, Z., Li, Z., Erb, A. and Schaaf, C. B.: Evaluation of the global MODIS 30 arc-
496 second spatially and temporally complete snow-free land surface albedo and reflectance
497 anisotropy dataset, *Int. J. Appl. Earth Obs. Geoinf.*, 58, 36–49, doi:10.1016/j.jag.2017.01.011,
498 2017.

499 Valin, L. C., Russell, A. R. and Cohen, R. C.: Variations of OH radical in an urban plume
500 inferred from NO₂ column measurements, *Geophys. Res. Lett.*, 40(9), 1856–1860, 2013.

501 Vasilkov, A., Qin, W., Krotkov, N., Lamsal, L., Spurr, R., Haffner, D., Joiner, J., Yang, E.-S.
502 and Marchenko, S.: Accounting for the effects of surface BRDF on satellite cloud and trace-gas
503 retrievals: a new approach based on geometry-dependent Lambertian equivalent
504 reflectivity applied to OMI algorithms, *Atmos. Meas. Tech.*, 10(1), 333–349, doi:10.5194/amt-
505 10-333-2017, 2017.

506 Warren, S. G. and Wiscombe, W. J.: A Model for the Spectral Albedo of Snow. II: Snow

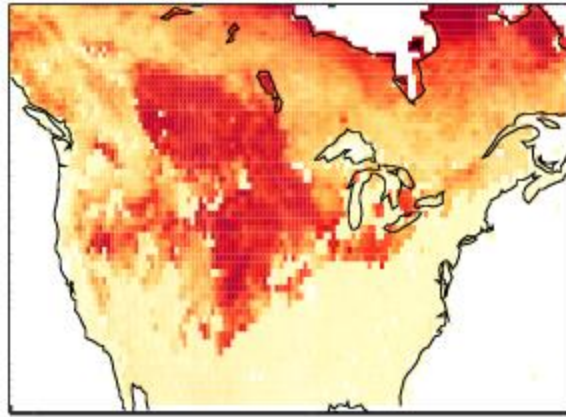
507 Containing Atmospheric Aerosols, *J. Atmos. Sci.*, 37(12), 2734–2745, doi:10.1175/1520-
508 0469(1980)037<2734:AMFTSA>2.0.CO;2, 1980.

509 Yang, J., Jiang, L., Ménard, C. B., Luo, J., Lemmetyinen, J. and Pulliainen, J.: Evaluation of
510 snow products over the Tibetan Plateau, *Hydrol. Process.*, 29(15), 3247–3260,
511 doi:10.1002/hyp.10427, 2015.

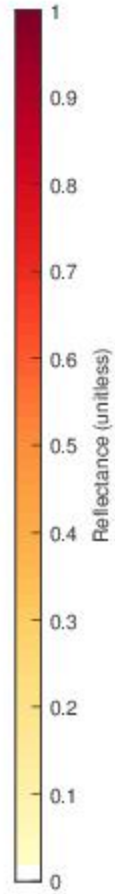
512 Zoogman, P., Liu, X., Suleiman, R. M., Pennington, W. F., Flittner, D. E., Al-Saadi, J. A.,
513 Hilton, B. B., Nicks, D. K., Newchurch, M. J., Carr, J. L., Janz, S. J., Andraschko, M. R., Arola,
514 A., Baker, B. D., Canova, B. P., Chan Miller, C., Cohen, R. C., Davis, J. E., Dussault, M. E.,
515 Edwards, D. P., Fishman, J., Ghulam, A., González Abad, G., Grutter, M., Herman, J. R., Houck,
516 J., Jacob, D. J., Joiner, J., Kerridge, B. J., Kim, J., Krotkov, N. A., Lamsal, L., Li, C., Lindfors,
517 A., Martin, R. V., McElroy, C. T., McLinden, C., Natraj, V., Neil, D. O., Nowlan, C. R.,
518 O’Sullivan, E. J., Palmer, P. I., Pierce, R. B., Pippin, M. R., Saiz-Lopez, A., Spurr, R. J. D.,
519 Szykman, J. J., Torres, O., Veefkind, J. P., Veihelmann, B., Wang, H., Wang, J. and Chance, K.:
520 Tropospheric emissions: Monitoring of pollution (TEMPO), *J. Quant. Spectrosc. Radiat. Transf.*,
521 186, 17–39, doi:10.1016/j.jqsrt.2016.05.008, 2017.

522

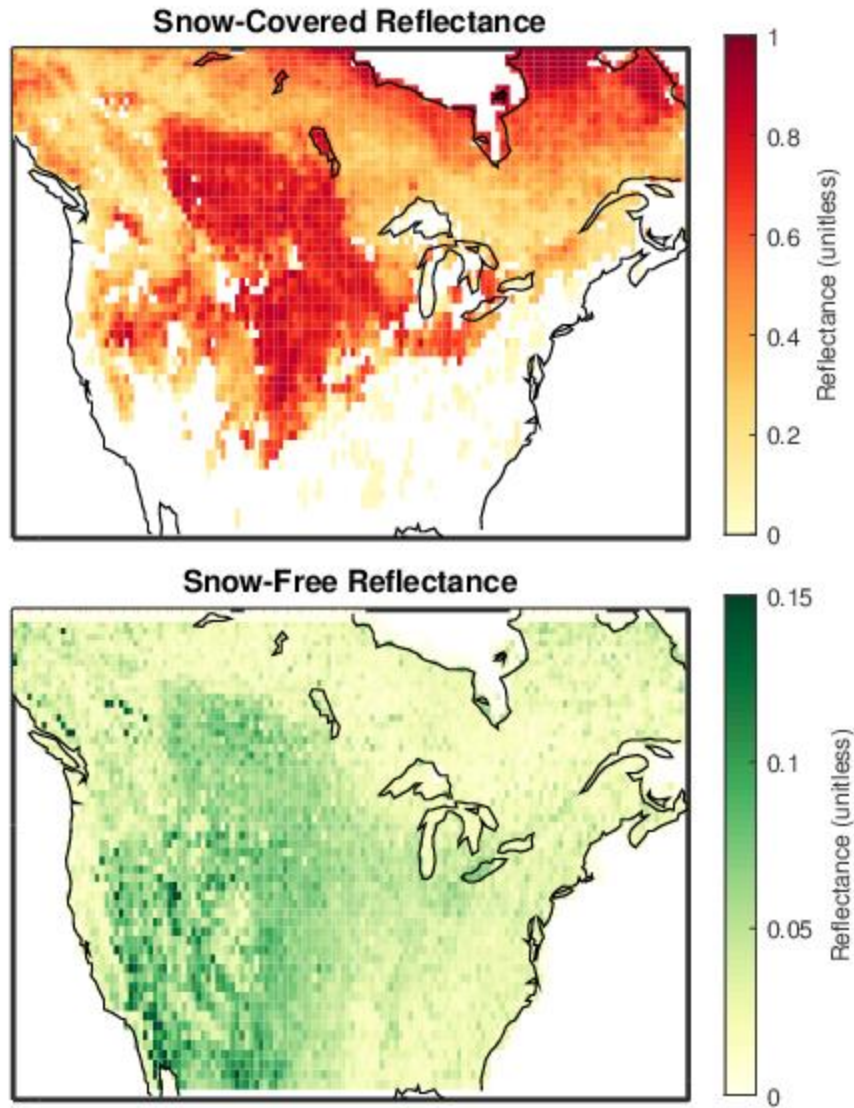
Snow-Covered Reflectance



Snow-Free Reflectance



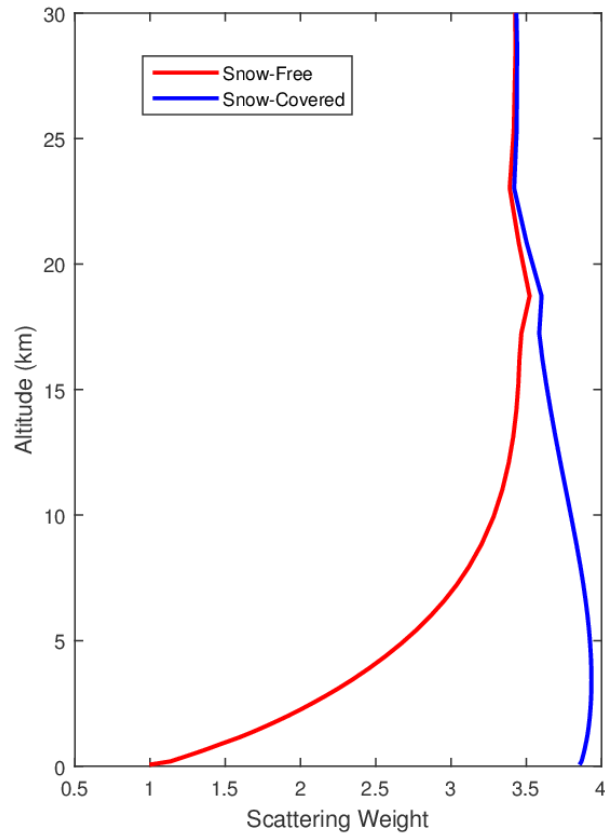
523



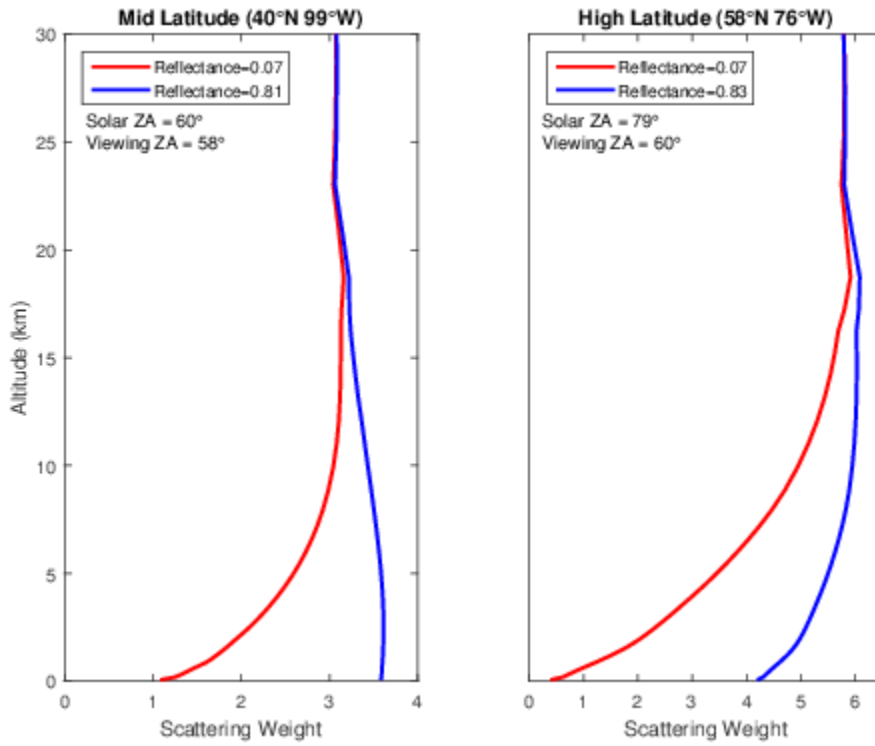
524

525 Figure 1: Surface reflectivity at UV-visible wavelengths for snow-covered and snow-free
526 conditions for January 2013. White space in top panel indicates no snow reflectance information
527 is available.

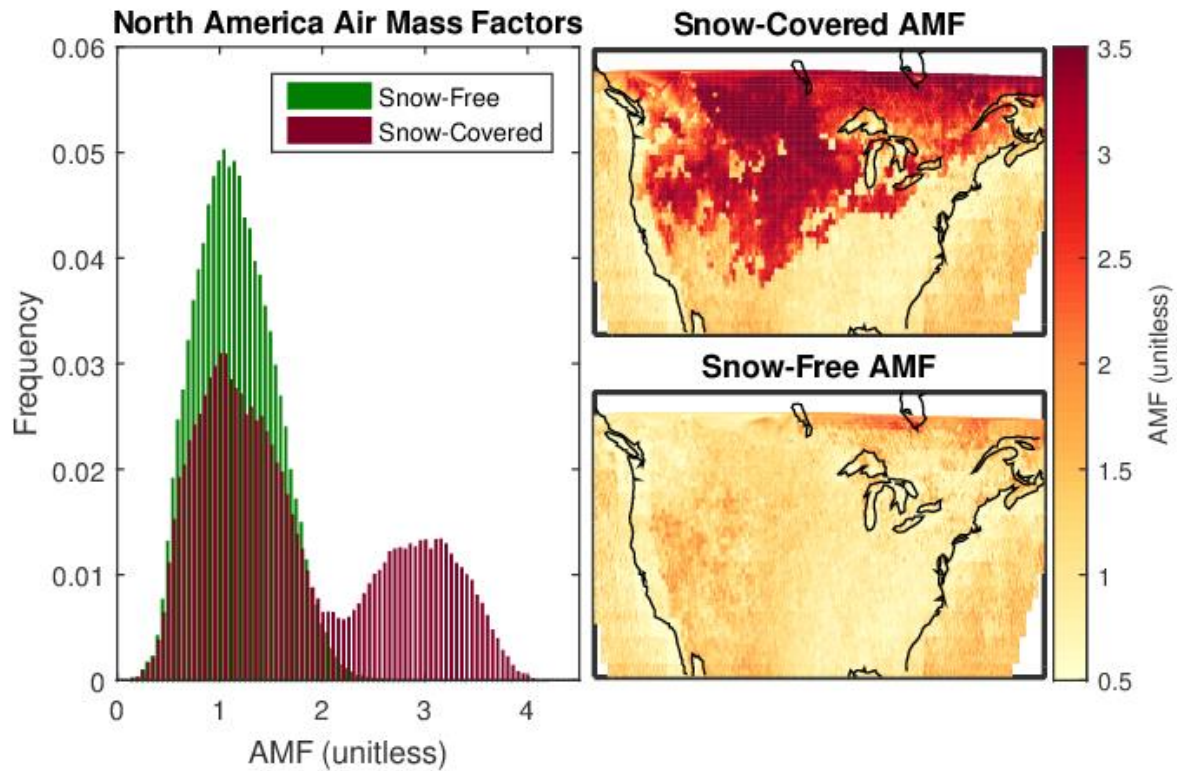
528



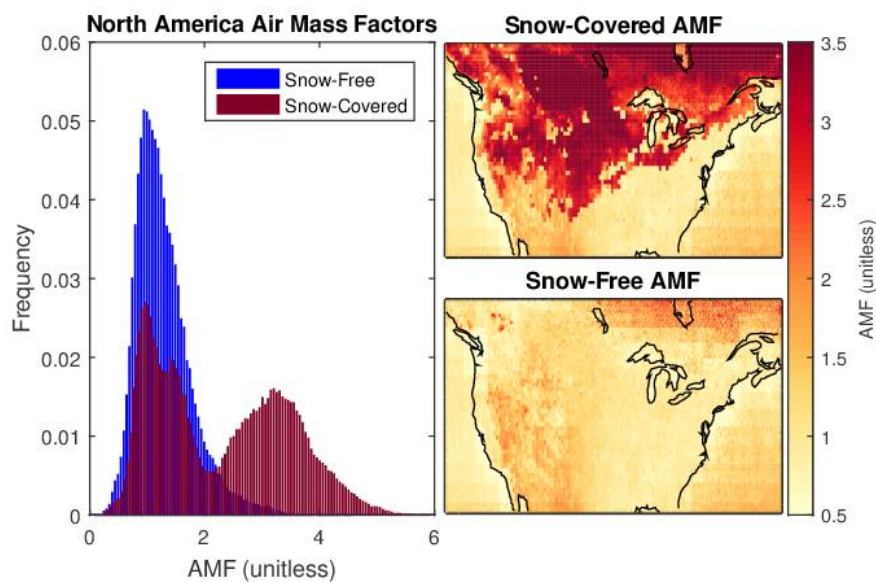
529



530 Figure 2: Observation sensitivity to NO₂. Scattering weight profiles calculated for cloud-free
531 OMI NO₂ retrievals, with and without surface snow cover, for January 2013 at (Left) 42° N,
532 10099° -W for January 2013 with a solar zenith angle (ZA) of 6560° and (Right) 58° N, 76° W
533 with a solar zenith angle of 79°.

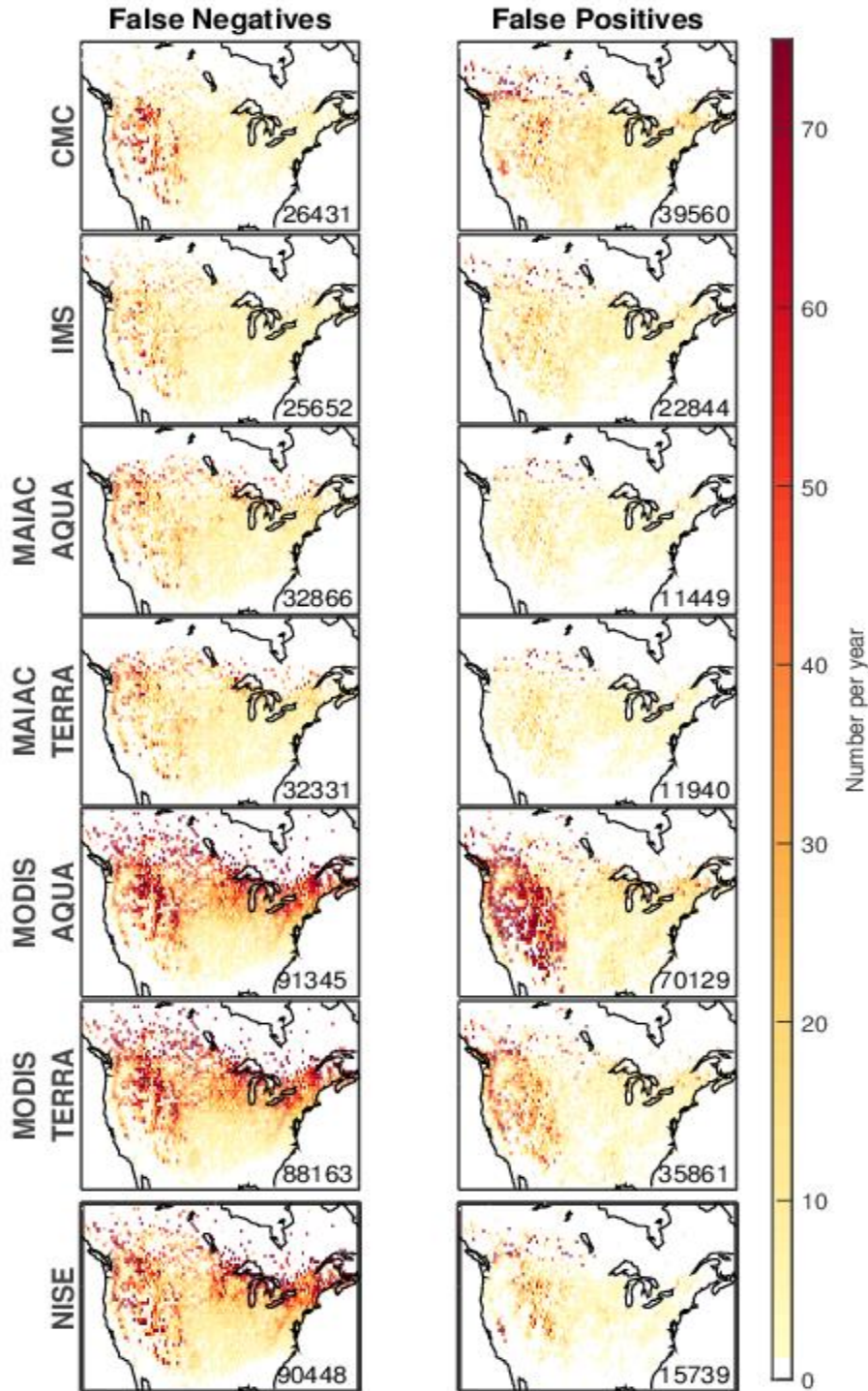


534



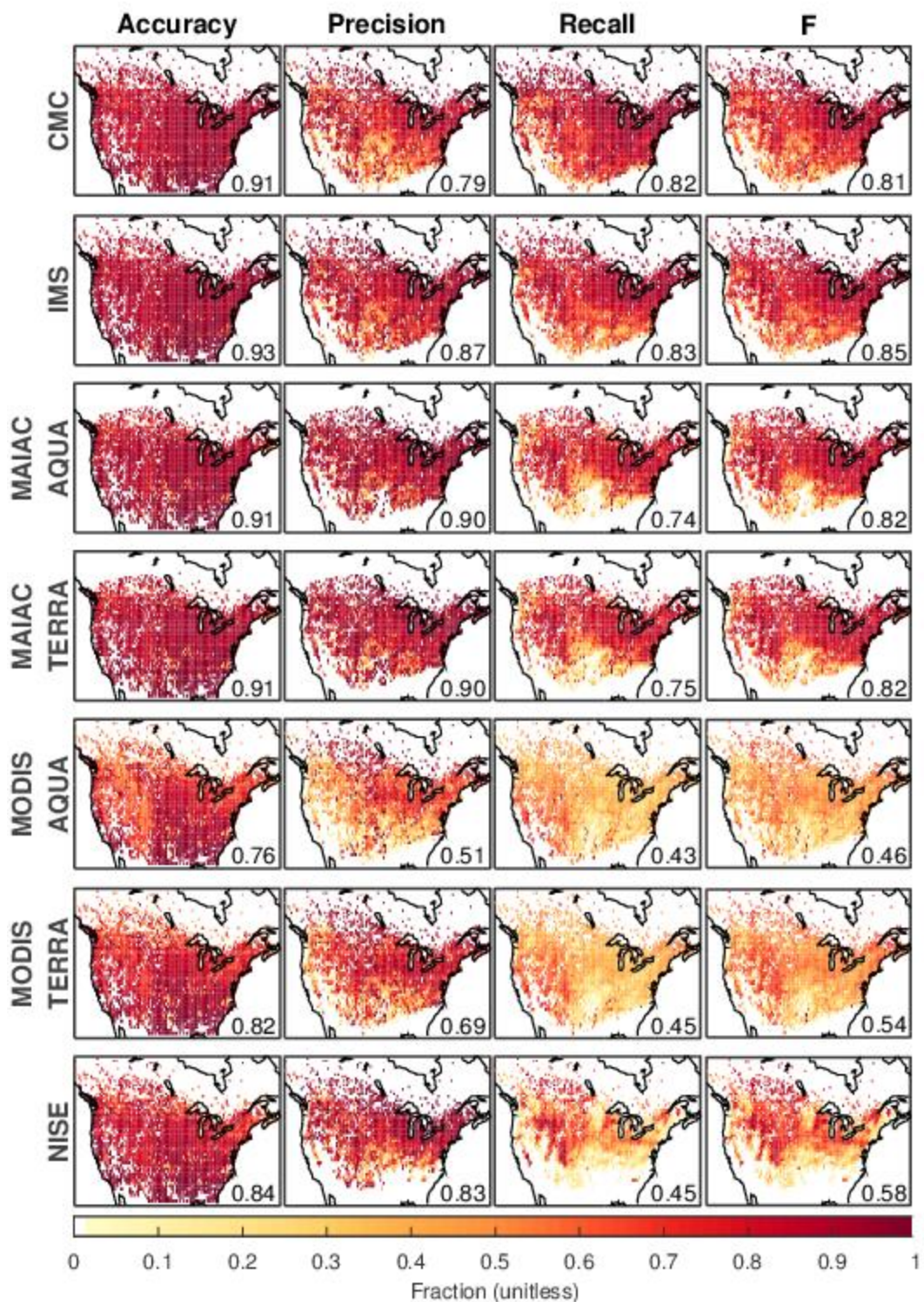
535

536 Figure 3: (Left) Distribution of Air Mass Factors (AMFs) calculated for OMI NO₂ retrievals over
 537 North America for observation geometry of January 2013, with and without surface snow cover.
 538 (Right) Maps of AMF for snow-covered and snow-free conditions.



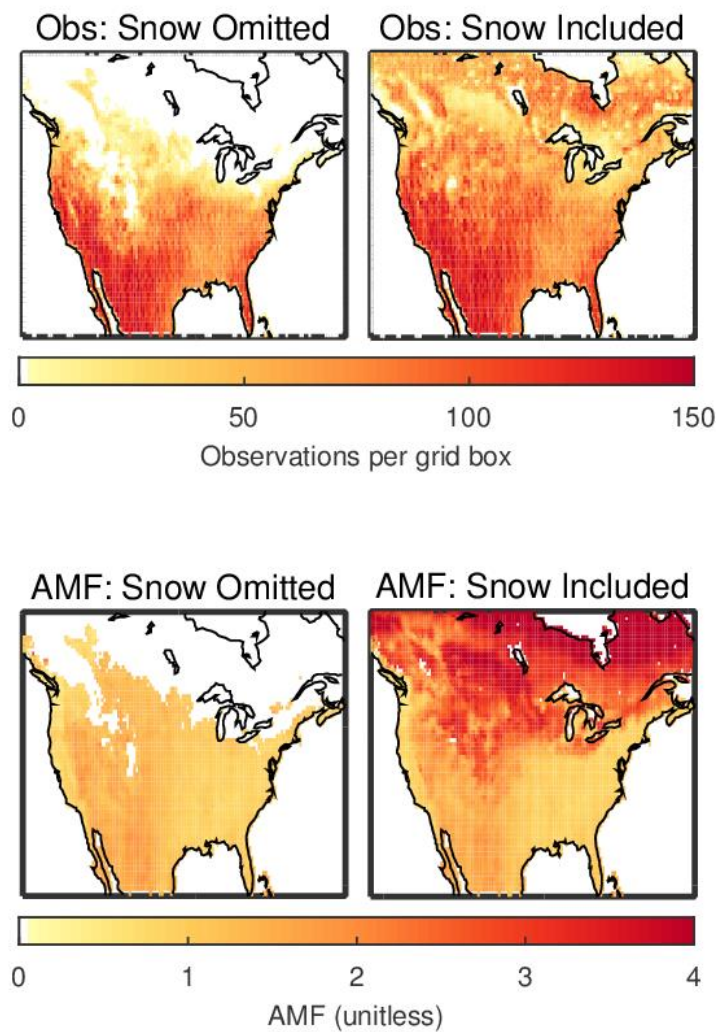
539

540 Figure 4: Number of false positive (FP) and false negative (FN) snow attributions by the snow
 541 data sets in 2015. All data sets are evaluated at 4 km resolution. Total number of false snow
 542 attributions inset. White space indicates no ground stations present.



543

544 Figure 5: Statistical metrics to evaluate snow cover products. All data sets are gridded at 4 km
 545 resolution. White space indicates no ground stations present.



546

547 Figure 6: OMI observation frequency (top) and average AMFs (bottom) over North America in
 548 January using IMS to identify surface snow conditions. White space indicates a lack of
 549 observations.

550

551

	Accuracy	Precision	Recall	F
CMC	0.91	0.79	0.83	0.81
IMS	0.93	0.87	0.83	0.85
MAIAC AQUA	0.91	0.90	0.74	0.82
MAIAC TERRA	0.91	0.90	0.75	0.82
MODIS AQUA	0.76	0.51	0.43	0.46
MODIS TERRA	0.82	0.69	0.45	0.54
NISE	0.84	0.83	0.45	0.58

552 Table 1: ~~Metrics for evaluating~~Evaluation of daily snow extent data set performance for 2015.

553 GHCN-D surface observations are used as “truth”. All products are regridded to a common 4 km
554 resolution. The highest value for each metric is shown in bold.

555 Appendix

<u>Months</u>	<u>Data Set</u>	<u>Accuracy</u>	<u>Precision</u>	<u>Recall</u>	<u>F</u>
<u>DJF</u>	<u>CMC</u>	<u>0.84</u>	<u>0.84</u>	<u>0.89</u>	<u>0.86</u>
	<u>IMS</u>	<u>0.88</u>	<u>0.90</u>	<u>0.88</u>	<u>0.89</u>
	<u>MAIAC AQUA</u>	<u>0.84</u>	<u>0.93</u>	<u>0.80</u>	<u>0.86</u>
	<u>MAIAC TERRA</u>	<u>0.84</u>	<u>0.92</u>	<u>0.80</u>	<u>0.86</u>
	<u>MODIS AQUA</u>	<u>0.58</u>	<u>0.84</u>	<u>0.34</u>	<u>0.48</u>
	<u>MODIS TERRA</u>	<u>0.60</u>	<u>0.88</u>	<u>0.37</u>	<u>0.52</u>
	<u>NISE</u>	<u>0.63</u>	<u>0.90</u>	<u>0.41</u>	<u>0.57</u>
<u>MAM</u>	<u>CMC</u>	<u>0.90</u>	<u>0.63</u>	<u>0.57</u>	<u>0.59</u>
	<u>IMS</u>	<u>0.93</u>	<u>0.74</u>	<u>0.67</u>	<u>0.70</u>
	<u>MAIAC AQUA</u>	<u>0.93</u>	<u>0.81</u>	<u>0.62</u>	<u>0.71</u>
	<u>MAIAC TERRA</u>	<u>0.93</u>	<u>0.81</u>	<u>0.63</u>	<u>0.71</u>
	<u>MODIS AQUA</u>	<u>0.86</u>	<u>0.43</u>	<u>0.39</u>	<u>0.41</u>
	<u>MODIS TERRA</u>	<u>0.89</u>	<u>0.62</u>	<u>0.40</u>	<u>0.49</u>
	<u>NISE</u>	<u>0.90</u>	<u>0.71</u>	<u>0.34</u>	<u>0.46</u>
<u>SON</u>	<u>CMC</u>	<u>0.91</u>	<u>0.73</u>	<u>0.81</u>	<u>0.76</u>
	<u>IMS</u>	<u>0.92</u>	<u>0.82</u>	<u>0.74</u>	<u>0.78</u>
	<u>MAIAC AQUA</u>	<u>0.91</u>	<u>0.86</u>	<u>0.60</u>	<u>0.71</u>
	<u>MAIAC TERRA</u>	<u>0.90</u>	<u>0.85</u>	<u>0.61</u>	<u>0.71</u>
	<u>MODIS AQUA</u>	<u>0.82</u>	<u>0.51</u>	<u>0.36</u>	<u>0.42</u>
	<u>MODIS TERRA</u>	<u>0.86</u>	<u>0.71</u>	<u>0.39</u>	<u>0.51</u>
	<u>NISE</u>	<u>0.85</u>	<u>0.85</u>	<u>0.25</u>	<u>0.39</u>

556 Table A1: Evaluation of daily snow extent data set performance by season for 2015. GHCN-D
557 surface observations are used as “truth”. All products are regridded to a common 4 km
558 resolution. The highest value for each metric/season is shown in bold.

559

560

	Resolution	Accuracy	Precision	Recall	F
CMC	25 km	0.92	0.81	0.81	0.81
IMS	4 km	0.93	0.87	0.83	0.85
MAIAC AQUA	1 km	0.91	0.91	0.71	0.80
MAIAC TERRA	1 km	0.91	0.90	0.71	0.80
MODIS AQUA	0.05°	<u>0.7977</u>	<u>0.7950</u>	<u>0.4430</u>	<u>0.4937</u>
MODIS TERRA	0.05°	<u>0.8081</u>	<u>0.7965</u>	<u>0.4732</u>	<u>0.2843</u>
NISE	25 km	0.85	0.87	0.37	0.51

561 Table ~~A1A2~~: Evaluation of Metrics for evaluating daily snow extent data set performance for
 562 2015. GHCN-D surface observations are used as “truth”. The highest value for each metric is
 563 shown in bold.

564

	Accuracy	Precision	Recall	F
CMC	0.92	0.81	0.8 <u>10</u>	0.8 <u>10</u>
IMS	0.93	0.84	0.854	0.84
MAIAC AQUA	0.87	0.69	0. <u>6973</u>	0. <u>6971</u>
MAIAC TERRA	0.8 <u>87</u>	0.68	0. <u>6873</u>	0. <u>6871</u>
MODIS AQUA	0.78	0. <u>5049</u>	0.41	0.45
MODIS TERRA	0.83	0.68	0.43	0.53
NISE	0.85	0.8687	0.37	0. <u>5452</u>

565 Table ~~A2A3~~: Metrics for evaluating Evaluation of daily snow extent data set performance for
 566 2015. GHCN-D surface observations are used as “truth”. All products are regridded to a common
 567 25 km resolution. The highest value for each metric is shown in bold.